ROYAL SOCIETY OF CHEMISTRY

EDGE ARTICLE

Check for updates

Highly selective and AI-predictable Se−N exchange chemistry between benzoselenazolones and boronic acids for programmable, parallel, and DNA-encoded library synthesis

Wei Zhou,†[a] Yan Wang,†[b] Shuning Zhang, [ID] †[c] Chengwei Zhang,†[d] Jiacheng Pang,[a] Shaoneng Hou,[a] Jie Li,[b] Ying Yao,[b] An Su, [ID] *[a] Peixiang Ma, [ID] *[c] Hongtao Xu [ID] *[b] and Wei Hou [ID] *[a]

Chemical reactions compatible with multiple functionalities are essential for rapid, programmable, and automatable synthesis of functional molecules. However, achieving such reactivity poses significant challenges. Here, we developed a novel multi-orthogonal C(sp²)−Se bond formation reaction between benzoselenazolones and boronic acids *via* Ag(I)-catalyzed selective selenium(II)−nitrogen exchange. This chemistry is compatible with diverse functionalities, enabling sequential and programmable synthesis. Moreover, it features modular, high-yielding (485 examples, with yields or conversions exceeding 70% in 95% of cases), and switchable reaction systems under mild conditions. Its practical utility was exemplified through late-stage functionalization of natural products, peptide modification and ligation, diversified synthesis, sequential click chemistry, protecting group-free syntheses of sequence-defined oligo selenides (nonamers), on-plate nanomole-scale parallel synthesis (200 nmol, 412 selenides), and DNA-encoded library (DEL) synthesis (10 nmol, 92 examples). Notably, a target-based screening identified **SA-16** as a potent CAXII inhibitor with an IC_{50} value of 72 nM. Furthermore, a machine learning-based model (SeNEx-ML) was established for reaction yield prediction, achieving 80% accuracy in binary classification and 70% balanced accuracy in ternary classification. These results demonstrated that this chemistry serves as a powerful tool to bridge the selenium chemical space with the existing chemical world, offering transformative potential across multidisciplinary fields.

Introduction

Selenium (Se) is an essential and unique trace element for human health.[1] Nature produces selenocysteine (Sec) in living organisms with 25 selenoproteins utilizing Sec as an integral component to participate in a wide range of physiological processes.[2] In addition to selenoproteins, incorporation of Se into small molecules has also been reported to enhance bioactivities *in vitro* and *in vivo*, including antioxidant,[3] anti-tumor,[4,5]

and anti-multidrug resistance activities,[6,7] just to name a few[8,9] (Fig. 1a). As a result, the design and synthesis of organic Se (Org-Se) compounds to prevent and treat diseases has attracted considerable interest in recent years.[10–12] In the field of drug discovery, natural products (NPs) play a pivotal role as invaluable resources for identifying hit or lead compounds. However, nature's biosynthetic pathways primarily prioritize the incorporation of selenium into protein and nucleic acid biopolymers[13] rather than seleno-small molecules, making it exceedingly challenging to obtain seleno-lead compounds from natural sources.[14] Besides, the synthetic toolbox for Org-Se is significantly less developed compared to their sulfur counterparts.[15,16] These limitations have led to the fact that research on Org-Se therapeutic agents is still in its nascent stage.

Programmable synthesis is an emerging synthesis pattern that has attracted significant attention due to its great potential in the alterable and tunable synthesis of advanced functional small molecules, oligomers, and polymers.[17] As depicted in Fig. 1b, it primarily contains two patterns. The first pattern involves the successive functionalization of the multiple functionalities decorated on the starting substrates by leveraging

[a] Zhejiang Key Laboratory of Green Manufacturing Technology for Chemical Drugs, College of Pharmaceutical Science & Green Pharmaceutical Collaborative Innovation Center of Yangtze River Delta Region, Zhejiang University of Technology, Hangzhou 310014, China. E-mail: ansu@zjut.edu.cn; houwei@zjut.edu.cn

[b] Shanghai Institute for Advanced Immunochemical Studies & School of Life Science and Technology, ShanghaiTech University, Shanghai 201210, China. E-mail: xuht@shanghaitech.edu.cn
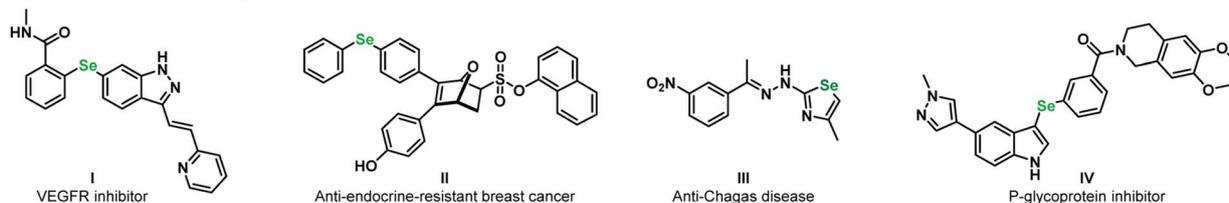
[c] Shanghai Key Laboratory of Orthopedic Implants, Department of Orthopedic Surgery, Shanghai Ninth People's Hospital, Shanghai Jiao Tong University, School of Medicine, Shanghai 201210, China. E-mail: mapx@shsmu.edu.cn

[d] College of Chemical Engineering, Zhejiang University of Technology, Hangzhou 310014, China
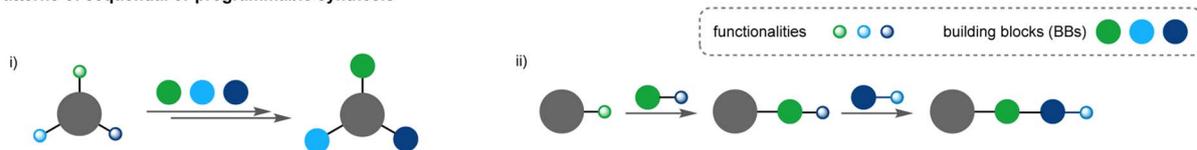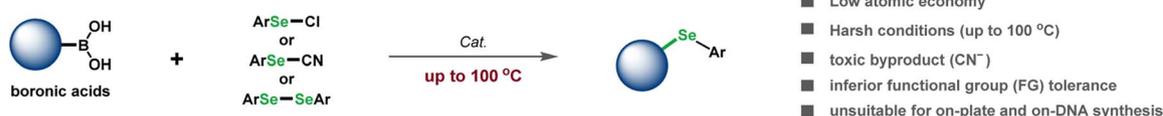
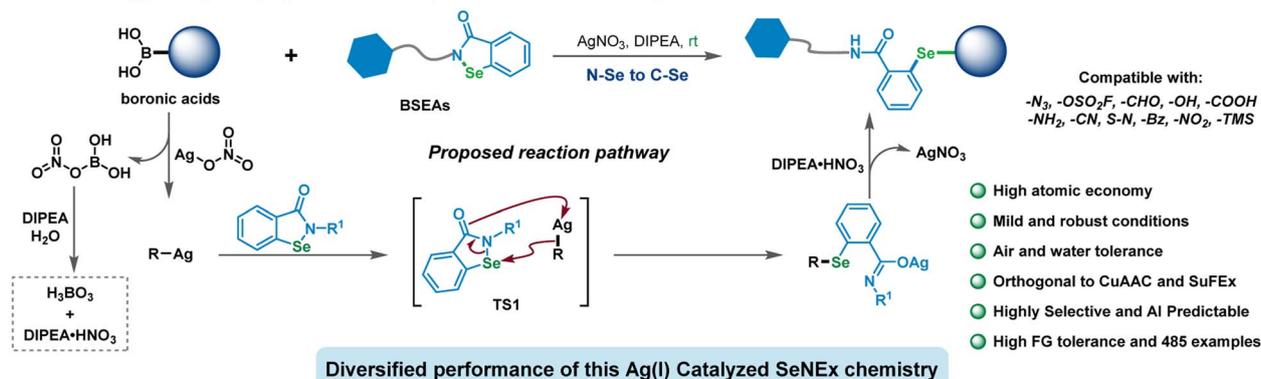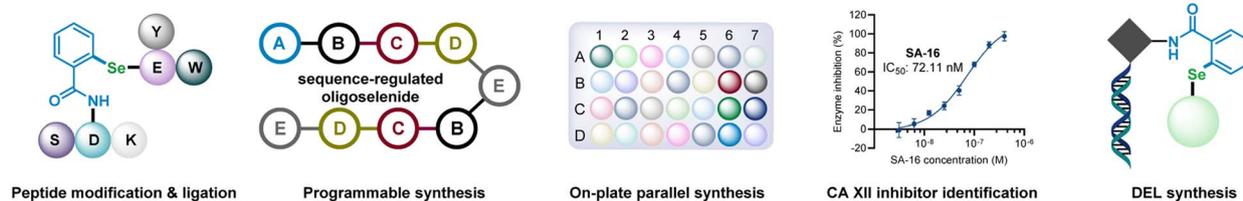† These authors contributed equally to this work.

Fig. 1 Representative organo-Se compounds and highly selective SeNEx chemistry between benzoselenazolones and boronic acids. (A) Representative bioactive organic Se compounds. (B) Patterns of sequential or programmable synthesis. (C) Previous work: boronic acid based C(sp^2)–Se bond formation chemistry. (D) This work: Ag(ı) catalyzed highly selective and AI predictable SeNEx chemistry between BSEA and boronic acid.

their distinct reactivity,[18,19] while the second pattern entails iterative building block (BB) connecting reactions, wherein the requisite functionalities for the subsequent connecting reaction are introduced in preceding steps.[20–22] Both patterns heavily rely on multi-orthogonal reactions with the ability to selectively functionalize one handle while preserving the others, which is quite challenging. Therefore, only a limited number of such syntheses have been reported to date. To meet the ever-growing demands for constructing advanced Org-Se compound libraries with expanded chemical space,[23] there is an urgent need for a synthetic toolbox that enables rapid, modular, and potentially automatable access to structurally diverse Org-Se compounds. In this context, despite the challenges, the development of highly selective and predictable selenylation chemistry capable of programmable functionalization of building blocks (BBs) bearing multiple transformable handles without the requirement for mandatory protection/deprotection becomes an important and appealing task. This will not only enrich the synthetic toolbox of multi-orthogonal selenylation chemistry but also hold great significance for seleno-medicinal chemistry and chemical biology.[24–26]

Inspired by the biochemical reaction between ebselen and cysteine (Cys) residues,[27,28] our group has designed benzoselenazolone (BSEA, the core structure of ebselen) as a novel bifunctional Se source for efficient selenylation reaction development. Based on the robust performance of these reactions, we have put forward the concept of Se(II)–N exchange (SeNEx) chemistry, which encompasses substitution events at an electrophilic Se(II) center to break Se–N bonds, enabling the rapid and flexible formation of Se–X bonds, especially Se–C bonds around the Se(II) center.[29–31] Especially, by leveraging the SeNEx strategy, we have developed several C(sp²)–Se bond formation reactions by employing in situ formed C(sp²)–Rh(III) species[32] and free indole as nucleophiles,[33,34] respectively. However, flaws such as elevated temperature requirements[32] and relatively narrow substrate scope (limited to indole and electron-rich aromatic rings)[33,34] have restricted their application in large-scale library construction while hindering the exploration of broader seleno-chemical space. To overcome these obstacles, we hypothesized that boronic acid would serve as an ideal coupling partner due to its ability to undergo a transmetalation under mild conditions,[35] generating nucleophilic carbon–metal species that are less reliant on the electric properties of aromatic rings (Fig. 1d). Notably, although selenylation reactions between aryl boronic acids and some Se electrophiles (e.g., selenyl chloride,[36] diselenide,[37] and selenocyanate[38]) have been reported, these methods typically suffer from some intrinsic drawbacks, such as poor atom economy, harsh conditions (up to 100 °C), toxic byproduct (CN⁻) and poor functional group tolerance, which hindered their practical application in large-scale library construction such as on-plate parallel synthesis (Fig. 1c). Therefore, a mild, general and multi-orthogonal C(sp²)–Se bond formation chemistry is still highly desirable and can be devised from commercially available boronic acids and readily available BSEAs[39] via a SeNEx strategy.

However, three significant challenges need to be addressed:

(i) Achieving multi-orthogonality and high chemo-selectivity on Se–N over a wide range of competitive electrophiles, including ester, ketone, –CHO, –SO₂F, S–N, –NO₂, –N₃ and –CN;

(ii) Potential protodeboronation issue in the presence of H₂O and certain groups with active hydrogen such as –COOH, –OH, –NH₂, amide, and unprotected heterocycles;

(iii) Coordination interference caused by the Se atom and adjacent amide group in the product leading to reduced catalyst reactivity.

We proposed that these formidable intractable obstacles can be overcome through fine-tuning the catalytic systems. Herein, we present an unprecedented multi-orthogonal SeNEx chemistry between BSEAs and boronic acids via Ag(I) catalysis, which features modular, predictable, robust, high-yielding, mild and switchable reaction conditions and is operationally simple and orthogonal to a broad scope of reactive handles, such as carboxylic acids, free amines, azides, sulfonyl fluorides, silanes, aromatic (pseudo)halogens, and others, thus allowing this chemistry to be orthogonal to copper-catalyzed azide–alkyne cycloaddition (CuAAC),[40] sulfur–fluoride exchange (SuFEx),[41] and nearly all top 20 reactions in medicinal chemistry (e.g., amide bond formation and cross-coupling),[42] enabling the

sequential and programmable synthesis of advanced org-Se compounds efficiently when combined with other established reactions. The practical application was successfully demonstrated through natural product and peptide modification, multi-orthogonal and programmable synthesis, on-plate nanomole-scale parallel synthesis, and DEL synthesis (Fig. 1d).

Results and discussion

Reaction profile of SeNEx chemistry between BSEAs and boronic acids

To initiate our proof-of-concept studies, we chose N-ethyl benzoselenazolone (A1) and electron-deficient 4-fluoro-phenylboronic acid (B1) as template substrates for reaction condition optimization. As illustrated in Fig. 2 (entries 1–6) and SI (Table S1), a screening of catalysts, bases, and ligands showed that Pd(OAc)₂, [Rh(COE)₂Cl]₂ and Cu(OAc)₂ are inferior catalysts for this reaction (30–55%), while AgNO₃ and CuI are more favorable, affording the desired product (1) rapidly at room temperature in 95% and 92% yields, respectively (entries 1–6, Table S1). For the AgNO₃ catalytic system, the base is a key additive for this reaction. Both inorganic (K₂CO₃ and KF) and organic (DIPEA and Et₃N) bases can promote this reaction efficiently (92–98%, Table S1, entries 2 and 6–14). To our delight, the reaction solvents are quite switchable; both polar protic (EtOH and iPrOH), aprotic (EA, DCE, and DMA) and even aqueous solvents (EA : H₂O = 2 : 1, double-distilled H₂O and borate buffer (pH 9.4)) are workable (90–95%, Table S1, entries 15–19 and 39–40). Importantly, this reaction could also give good conversions when conducted at 10 times dilution (10 mM, Table S1, entry 20) or in miniaturization (200 nmol, 4 mM, Table S1, entry 21), indicating its potential in nanomole-scale in situ drug screening library synthesis. For the CuI catalytic system, the ligand is a critical factor in promoting the transformation. 5,5′-Dimethyl-2,2′-bipyridine (L3) was the best ligand in the reaction (95%, Table S1, entries 22–28). Likewise, both polar protic (EtOH and iPrOH) and aprotic (EA, DMF, DMSO, and MeCN) solvents are feasible for this reaction (92–95%), while a mixed solvent system (96%, EA : DCM = 1 : 1) is the optimum (Table S1, entries 29–38).

With the established reaction conditions in hand, we next explored the substrate scope and generality (Fig. 2 and SI, Fig. S3). For BSEAs, N-substituents, including alkyl (1–7, 23–26, 17–18, and 69), aryl (8–12 and 27), heterocycles (13–16, 19–22, 27, 28, 71, and 72), were all well tolerated, affording the desired selenides in 66–99% yields. Besides, the electronic effect of substituents on the phenyl moiety of BSEAs is not obvious, and both electron-withdrawing groups (EWGs, 23–24 and 27–28) and electron-donating groups (EDGs, 25–26) are compatible, delivering the desired selenides in high to excellent yields (85–95%). Notably, the N-unsubstituted BSEA A58 is an inferior coupling partner in this reaction, affording the desired product 73 in a low yield (25%) under standard conditions. When conducted at 60 °C, the yield of 73 can be increased to 55%, and compound 74 was obtained in a satisfactory 95% yield when 2-naphthaleneboronic acid B80 was employed. For arylboronic acids, a broad scope of substituents regardless of their location

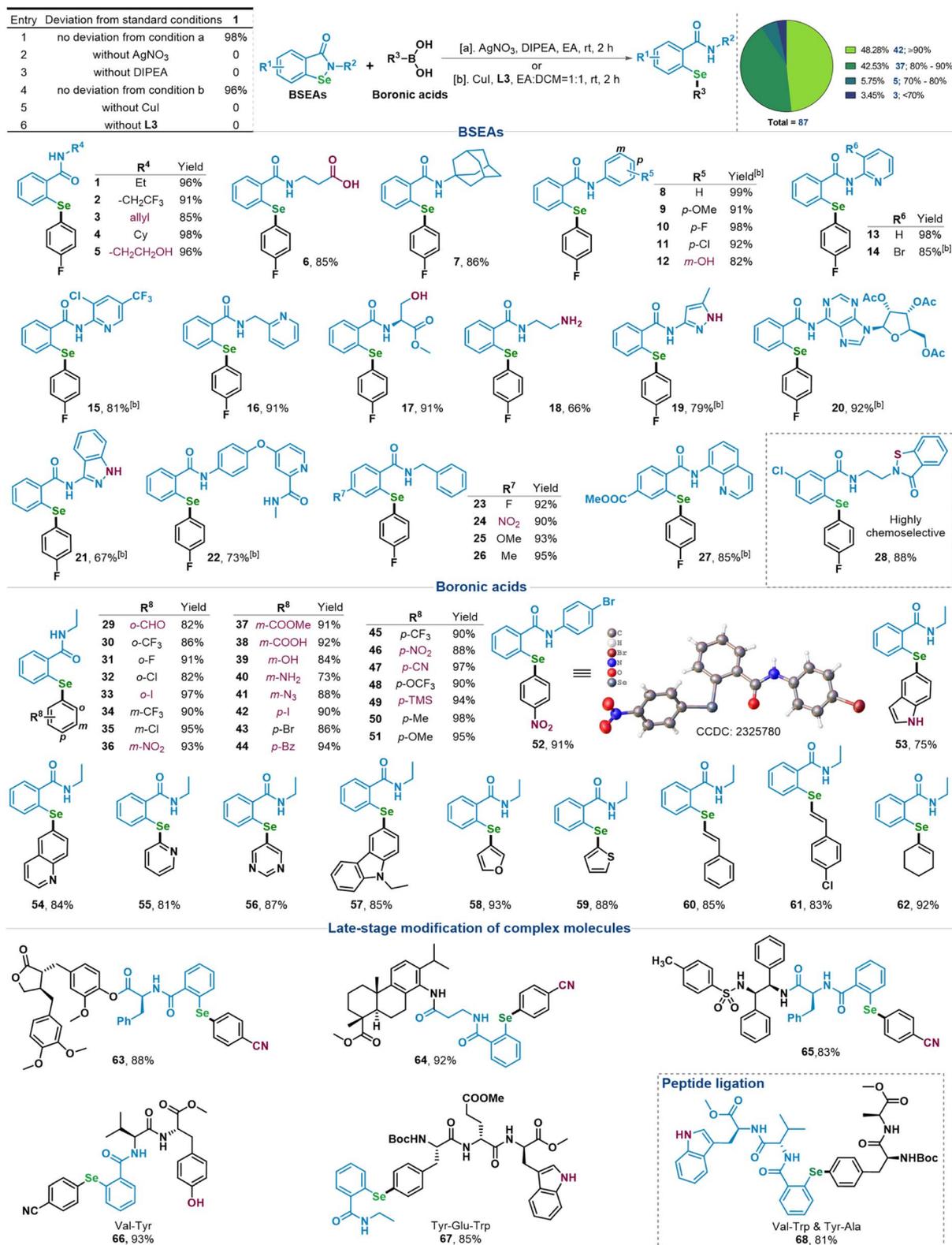**Fig. 2** Scope of the substrates. Standard conditions [a]: BSEA (0.2 mmol), boronic acid (0.24 mmol), DIPEA (0.3 mmol), and AgNO$_3$ (5 mol%) in EA (2 mL), rt, and 2 h (without air exclusion). Standard conditions [b]: BSEA (0.2 mmol), boronic acid (0.24 mmol), Cu I (5 mol%), and **L3** (5,5′-dimethyl-2,2′-bipyridine, 5 mol%) in EA : DCM = 1 : 1 (2 mL), rt, and 2 h (without air exclusion). Isolated yields are given.
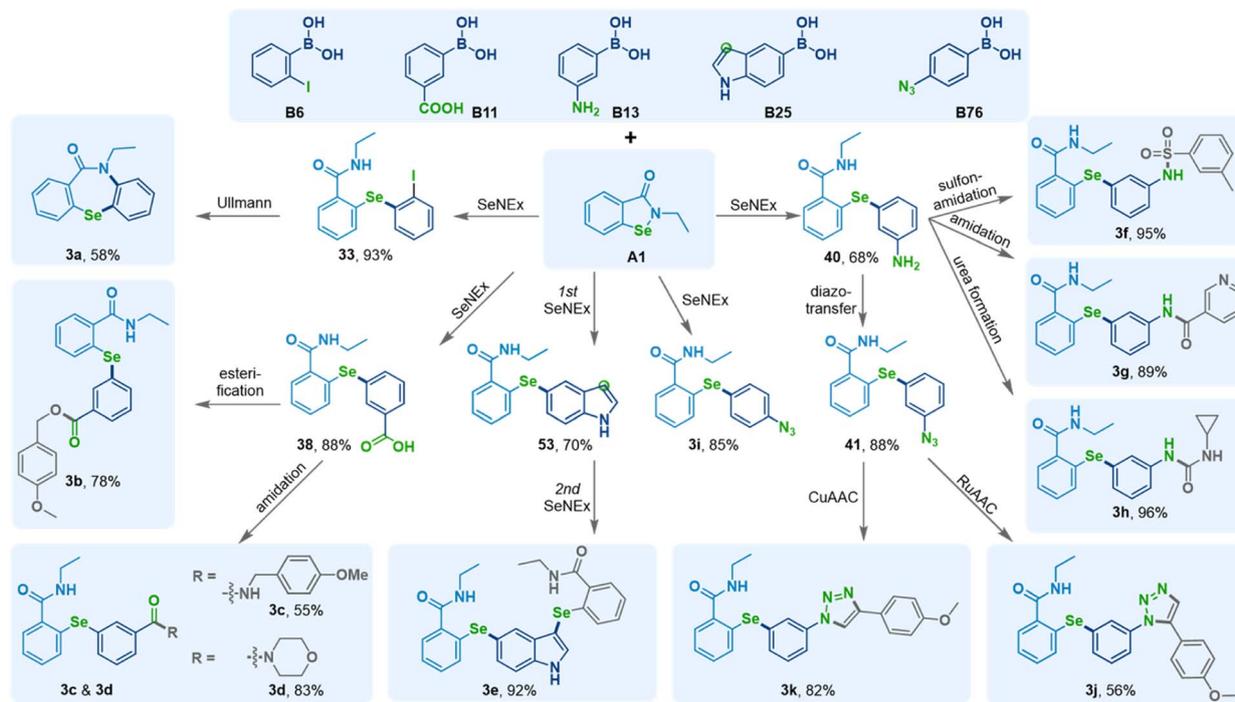
(*o*, *m*, and *p*) and electronic properties are all proved to be compatible coupling partners, delivering the corresponding selenides in good to excellent yields (**29–52** and **70**, 73–98%). To our delight, both heteroarylboronic acids (**53–59**) and alkenylboronic acids (**60–62**) underwent this SeNEx reaction favorably to furnish the corresponding products in 75–93% yields. The structure of **52** was unambiguously determined by X-ray crystal analysis. Notably, substrate **A28** orthogonally underwent this SeNEx click chemistry to afford the selenylation product **28** in 88% yield. At the same time, the benzo[*d*] isothiazolone (BITA) moiety in **28** is completely unaffected, albeit the potential electrophilicity of the S–N moiety. This excellent selectivity may originate from the larger size of Se than S, which results in a reduced orbital overlap, longer bond length, and weaker bond strength of Se–N than the S–N bond. The weaker bond strength indicates that the σ* orbital of the Se–N bond is lower in energy than that of the S–N bond, making BSEA Se more reactive than its S analog.[10] Significantly, this SeNEx reaction is also suitable for late-stage modification (LSF) of complex molecules, as exemplified by the efficient LSF of (−)-arctigenin (**63**, 88%) and dehydroabietic acid (**64**, 92%), the famous ligand (*R*,*R*)-TsDPEN (**65**, 83%), *S*-methyl cysteine (**75**), tryptophan (**76**), lysine (**77**), tyrosine (**78**), dipeptide Val–Tyr (**66**, 93%), Gly–Leu (**79**), Phe–Trp (**80**), Val–Trp (**81**), Tyr–Phe (**82**), Tyr–Lys (**83**), Tyr–Trp (**84**), Tyr–Ala (**85**), Tyr–Arg (**86**) and tripeptide Tyr–Glu–Trp (**67**, 85%) and Tyr–Asp–Ala (**87**, 88%). Impressively, two dipeptides bearing BSEA (Val–Trp) and boronic acid (Tyr–Ala) respectively can also undergo SeNEx smoothly to give the desired ligation product **68** in 81% yield, indicating its potential application in peptide ligation. Significantly, a broad scope of transformative functionalities and/or pharmacophores including terminal alkenyl (**3**), adamantyl (**7**), primary alcohol (**5** and **17**), phenol (**12** and **39**), carboxyl (**6** and **38**), free amine (**18** and **40**), pyridine (**13–16**, **22**, and **55**), pyrimidine (**56**), free pyrazole (**19**), 2′,3′,5′-tri-*O*-acetyl-D-adenosine (**20**), free indazole (**21**), azide (**41**), free indole (**53**), quinoline (**28** and **54**), carbazole (**57**), furan (**58**), thiophene (**59**), nitro (**24**, **36**, **46**, and **52**), ester (**27**, **37**, **63–64**, and **73**), amide (all cases), ketone (**44**), cyano (**47** and **63–65**), silyl (**49**), sulfonamide (**65**) and halo (**11**, **14**, **27**, **31–33**, **35**, **42**, and **43**) are all satisfactorily compatible, highlighting the excellent substrate scope of this SeNEx chemistry. It is noteworthy that many synthetic transformations suffer from a predicament in that polar and highly functionalized compounds fail to afford desired products, leading to the enrichment of hydrophobic compound sets, which are less likely to become successful drug candidates.[43] In contrast, the good tolerance of polar functionalities (*e.g.*, hydroxy, phenol, amine, carboxyl, pyridine, and pyrimidine) as well as complex natural products indicated that this SeNEx chemistry may cross this predicament. Moreover, the compatibility with terminal alkenyl, hydroxy, phenol, halogens (Cl, Br, and I), nitro, ester, ketone, silyl, free pyrazole, free indazole, free indole, –CHO, –OH, –NH$_2$, –N$_3$ and –COOH offers flexible and diverse handles for programmable synthesis.

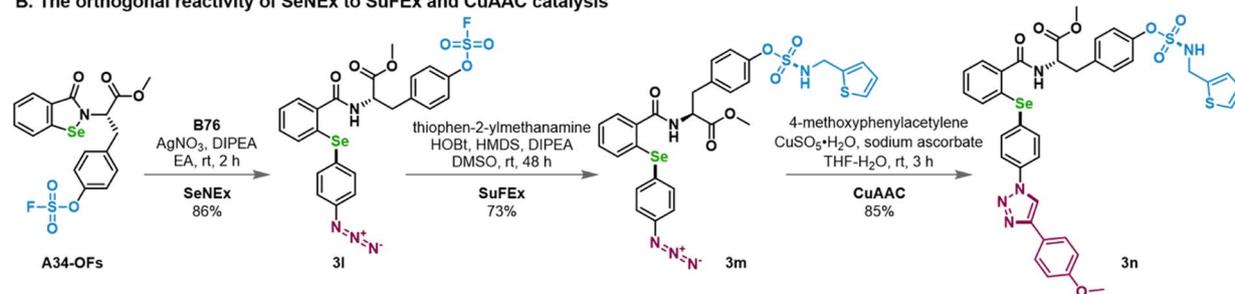## Multi-orthogonal and programable synthesis of advanced Org-Se compounds

The synthetic practicality of this Ag(I) catalyzed SeNEx chemistry was further demonstrated by gram-scale (5 mmol) synthesis of **33**, **38**, **40**, and **53** to afford them in 93%, 88%, 68%, and 70% yields, respectively (Fig. 3a). **33** underwent the intramolecular Ullmann coupling smoothly to deliver **3a** in 58% yield, which contains a new heterocycle scaffold dibenzo[*b*,*f*][1,4]selenazepine. Notably, considering that dibenzo[*b*,*f*][1,4]thiazepine is known as the core structure of the antipsychotic drug Clotiapine, its bioisostere dibenzo[*b*,*f*][1,4]selenazepine may also have the potential to be applied in the research and development of central nervous system (CNS) drugs. Besides, the compatibility with carboxyl and amino groups indicates that this SeNEx reaction is orthogonal to the basic and powerful ester and amide condensation and *N*-capping reactions (top 3 reactions in medicinal chemistry),[42] enabling controlled and programmable synthesis. For instance, **38** can be readily transformed to **3b** (esterification), **3c** (secondary amide), and **3d** (tertiary amide) in 78%, 55% and 83% yields, respectively. Likewise, the amino in **40** can be elaborated favorably to afford **3f** (sulfonamide), **3g** (amide), and **3h** (urea) in 89–96% yields. Moreover, this SeNEx reaction is also orthogonal to other known click chemistry and could be coupled with them efficiently, as exemplified by direct synthesis of azide substituted selenide (**3i**), dual SeNEx (**3e**), SeNEx–SuFEx–RuAAC (**3j**) and SeNEx–SuFEx–CuAAC (**3k**). Impressively, the fluorosulfate-modified BSEA (**A34-OFs**) reacted smoothly with azide-bearing boronic acid (**B76**) to afford **3l** in 86% yield, which further underwent accelerated SuFEx (**3m**, 73%) and CuAAC (**3n**, 85%) efficiently (Fig. 3b), demonstrating the good orthogonality of this SeNEx click chemistry to SuFEx and CuAAC. Moreover, a purification-free and one-pot three consecutive click sequence of SeNEx–SuFEx–SuFEx was conducted to exclusively produce the "multi-clicked" product **3o** in an excellent 90% HPLC purity and 85% yield over three steps (Fig. 3c). These programmable click sequences highlighted the potential of this SeNEx chemistry in *in situ* synthesis of Se-containing compounds with multi-dimensional diversity. Ultimately, a streamlined synthesis of Se-axitinib (**3q**)[9] (Fig. 3d), a seleno-analog of the FDA-approved second-generation tyrosine kinase inhibitor (TKI) for the treatment of renal cell carcinoma (RCC), has also been smoothly prepared by simple coupling of BSEA **A51** with the advanced boronic acid intermediate **B77** *via* this SeNEx chemistry and a following deprotection. Taken together, these preliminary rehearsals highlight the great potential of this SeNEx chemistry in the controlled and programmable synthesis of advanced Org-Se compounds with drug-like properties.

Reliable strategies for the controlled synthesis of sequence-defined oligomers and polymers, which have promising applications in materials chemistry and biological research, are uncommon but highly desirable.[22] Inspired by the good orthogonal reactivity of this Ag(I) catalyzed SeNEx chemistry to SuFEx, we next reason that SeNEx and SuFEx are ideal coupling reactions for building sequence-defined oligomers in a protecting group free and iterative-growth pattern. As illustrated in

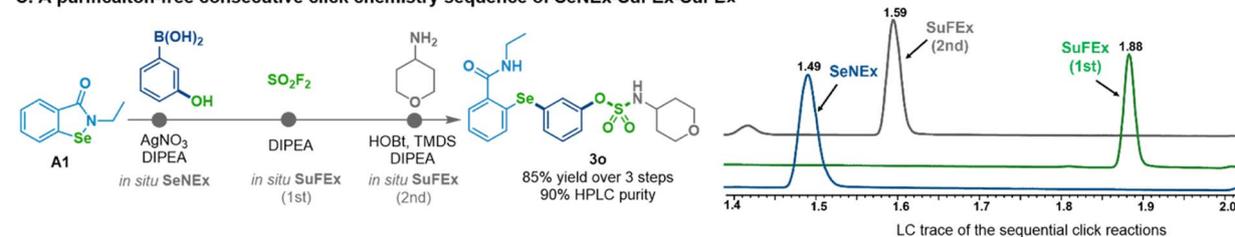**Fig. 3** Diversified synthetic application of this SeNEx chemistry. (A) The orthogonal reactivity of SeNEx to ArI, COOH, NH$_2$, indole and N$_3$-based elaboration. (B) The orthogonal reactivity of SeNEx with SuFEx and CuAAC catalysis. (C) A purification-free click chemistry sequence of SeNEx–SuFEx–SuFEx. (D) Streamlined synthesis of seleno-axitinib by using SeNEx chemistry as the key connection.
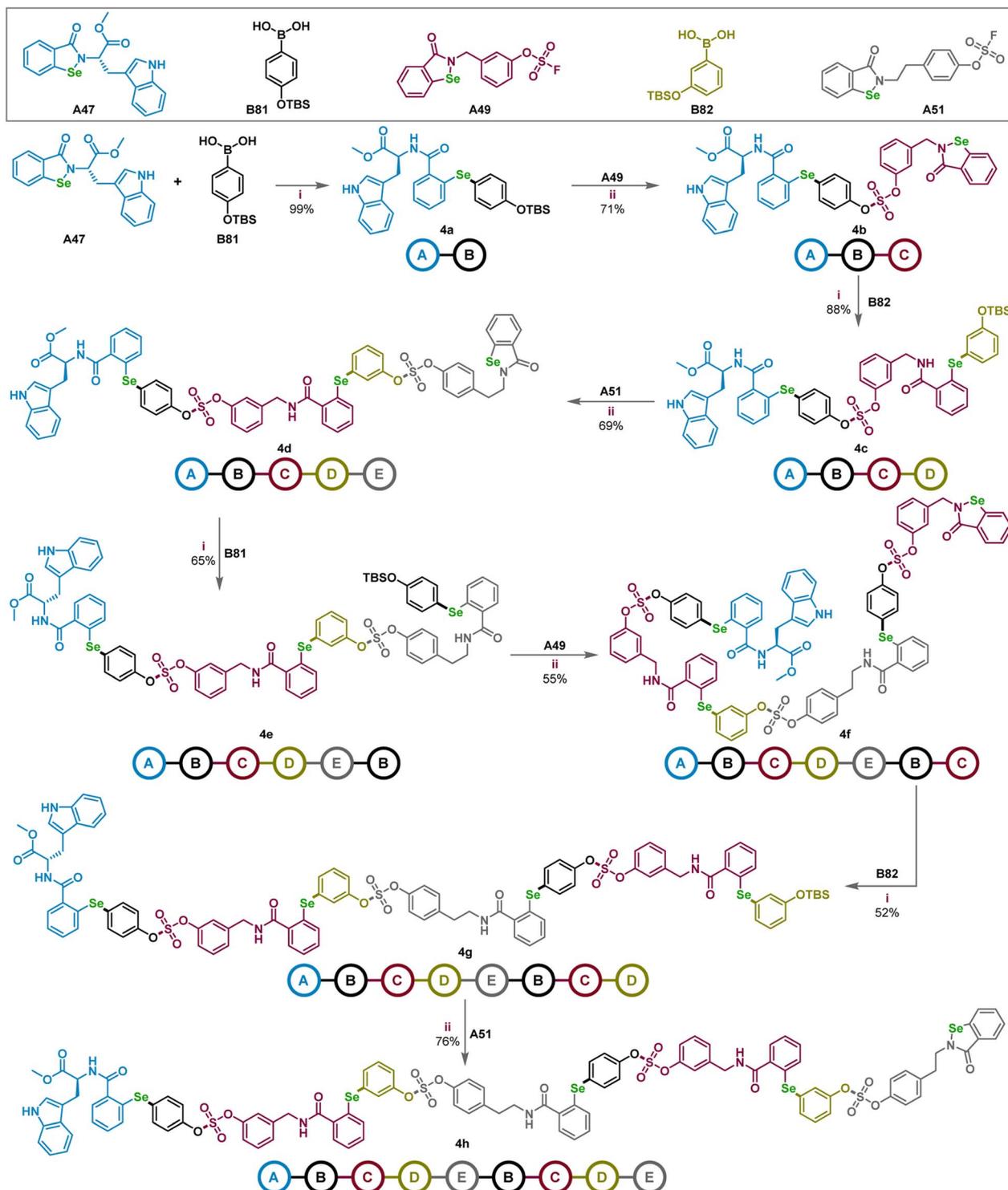
Fig. 4 Iterative SeNEx and SuFEx chemistries for the synthesis of sequence-defined oligo selenides. (i) SeNEx condition (a): BSEA (1.0 equiv.), boronic acid (1.2 equiv.), DIPEA (1.5 equiv.), AgNO₃ (5 mol%), EA, and rt. (ii): reactants (1.0 equiv.), 1,8-diazabicyclo-(5.4.0)undec-7-ene (DBU, 0.25 equiv.), MeCN, and 80 °C.

Fig. 4, we chose compound **A47** (a tryptophan derived BSEA), – OTBS containing phenylboronic acids (**B81** and **B82**) and fluorosulfate-modified BSEAs (**A49** and **A51**) as coupling monomers for the programmable nonamer synthesis. Trimer **4b** (A–B–C) was first prepared in 71% yield over two steps from

SeNEx between **A47** and **B81** and then SuFEx with **A49**. Next, a second round of the SeNEx–SuFEx reaction sequence involving **4b, B82,** and **A51** afforded the desired pentamer **4d** (A–B–C–D–E) in 60.7% yield over two steps. Starting from **4d** and repeating this SeNEx–SuFEx–SeNEx–SuFEx reaction sequence

ultimately delivered the desired oligo-selenide **4h** (nonamer, A–B–C–D–E–B–C–D–E) in 14% yield over four steps, containing a BSEA group for potential further chain growth. Overall, the successful generation of the nonamer once again confirms the good orthogonality between SeNEx and SuFEx, and it also confirms the good feasibility of combining SeNEx with SuFEx to build sequence-defined oligomers in a protecting group free fashion. In addition, the investigation of combining SeNEx with SuFEx to prepare sequence-defined polymers will be a focus of our future research.[21]

Nanomole-scale synthesis—parallel synthesis and DNA-encoded library synthesis

Miniaturization of organic reactions to a nanoscale is becoming more and more important for accelerating the discovery of hit or lead compounds,[44] because *in situ* nanomole-scale combinatorial compound libraries possess significant advantages over traditional compound libraries, including less material consumption to generate more products and more reaction data, less waste production, and the ability to be used for direct
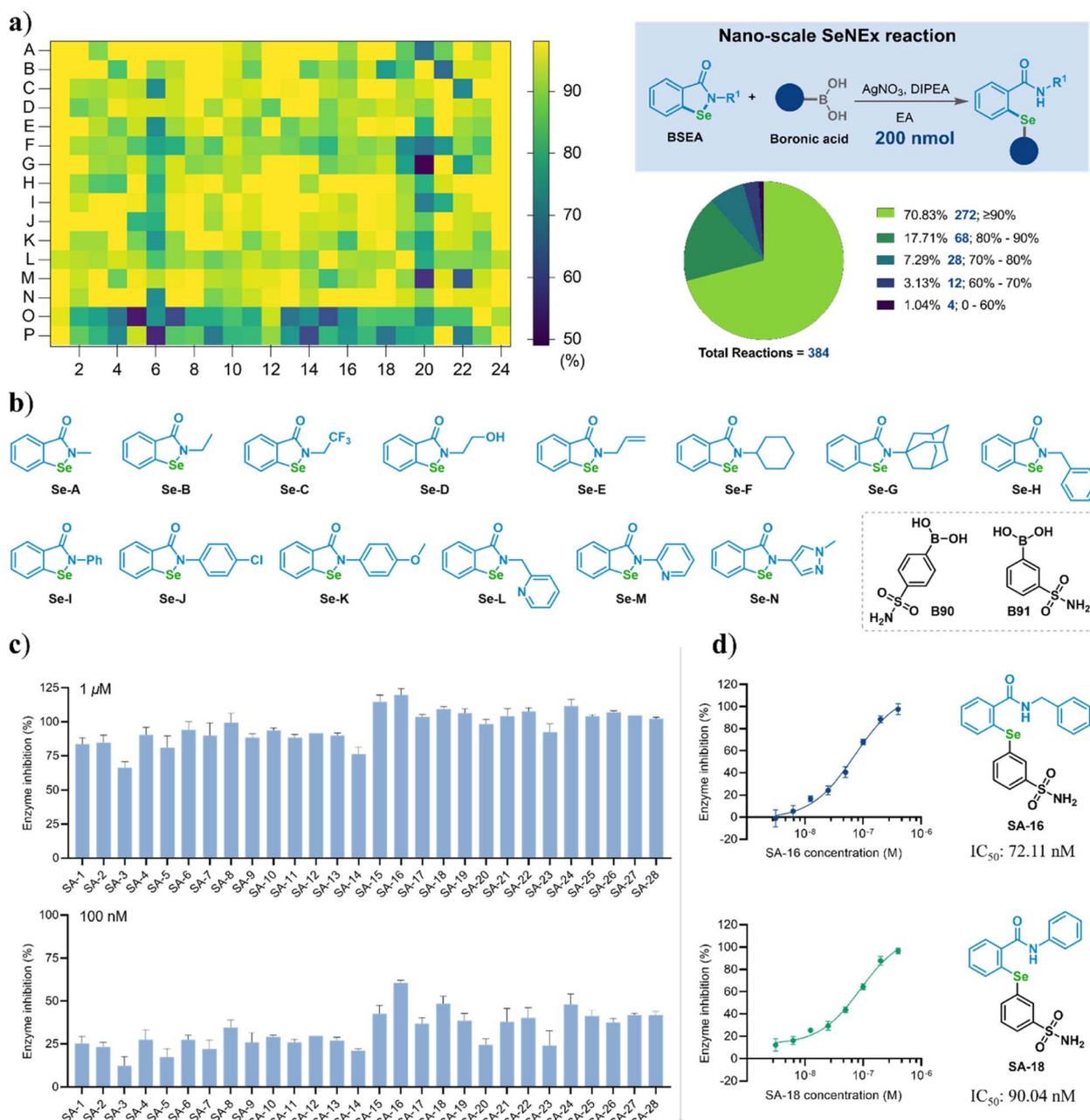
Fig. 5 On-microplate nanomole-scale parallel synthesis enables efficient identification of novel CA XII inhibitors. (a) 16 × 24 nanomole-scale parallel synthesis on 96-well microplates. (b) 14 × 2 nanomole-scale parallel synthesis on 96-well microplates. (c) Inhibitory rates of 28 compounds against CA XII at 1 μM and 100 nM. (d) IC_{50} determination of **SA-16** and **SA-18**; each experiment was run three times independently (n = 3). Standard condition of parallel synthesis: BSEAs (200 nmol), boronic acids (200 nmol), DIPEA (300 nmol), and AgNO₃ (5 mol%) in EA (50 μL), 50 °C, and 6 h (without air exclusion). Conversions are determined by LC-MS analysis. LC-MS, liquid chromatography-mass spectrometry.

biological screening without purification of the crude products.[45] Meanwhile, their construction requires reactions with high yield, good predictability, mild reaction conditions, and reliable performance at the nanomole scale in microliter-scale reaction droplets.[43,46] However, most of the synthetic "toolbox" cannot be readily miniaturized. Consequently, the development of new reactions suitable for nanomole-scale parallel synthesis is of great significance.

Encouraged by the robust performance and high yields of this SeNEx chemistry as well as our previous experience in on-plate parallel synthesis,[29,33,34] we subsequently performed a nanomole-scale parallel synthesis on 96-well microplates via the combination of 16 BSEAs and 24 boronic acids (16 × 24, 200 nmol, 4 mM, Fig. 5 and SI, Fig. S4 and S5). From the perspective of molecular diversity, the selected 16 BSEAs contain alkyl (Se-A–Se-G), aryl (Se-H–Se-K), heteroaryl (Se-L–Se-N), and amino acid (Se-O and Se-P) side chains. Meanwhile, the selected 24 boronic acids contain ortho- (BA-2–BA-4), meta- (BA-5–BA-9), para-substituted (BA-10–BA-19), electron-neutral (BA-1), EWGs (BA-2, BA-3, BA-7–BA-9, and BA-12–BA-19), EDGs (BA-4–BA-6, BA-10, and BA-11), electron-rich heterocycles (BA-21–BA-23), electron-deficient heterocycles (BA-20), and alkenyl (BA-24), respectively. The conversions were analyzed by liquid chromatography-mass spectrometry (LC-MS). Among the 384 selenides, 272 (70.8%) attained >90% conversion and 368 (95.8%) achieved >70% conversion—a generally accepted threshold for in situ biological screening[47,48] (Fig. 5a). Notably, all of the 384 selenides are new structures; therefore, they could further enrich the Org-Se chemical space. In addition, it is reported that carbonic anhydrase XII (CA XII), a tumor-associated membrane protein applicable for hypoxic tumor therapy and imaging, can be recognized by aromatic sulfonamides.[49,50] Given the good tolerance of this SeNEx reaction towards the sulfonamide group and to explore its potential in the discovery of bioactive molecules, we further conducted a parallel synthesis (14 × 2, 14 BSEAs and 2 sulfonamide-boronic acids, Fig. 5b) to search for novel CA XII inhibitors via in situ target-based screening. To our delight, 22 out of the prepared 24 compounds exhibited over 80% inhibition at 1 μM, and 3 out of the tested 24 compounds exhibited over 48% inhibition at 100 nM (Fig. 5c). Further resynthesis and IC_{50} determination indicated both SA-16 and SA-18 are potent CAXII inhibitors, with IC_{50} values of 72 nM and 90 nM, respectively (Fig. 5d). Overall, these positive results highlight the great potential of SeNEx chemistry in in situ nanomole-scale high-throughput medicinal chemistry. With the experimentally measured dataset comprising 447 reaction yields, we further developed a machine learning (ML)-driven reaction yield predicting model, termed SeNEx-ML, to forecast the yields of these reactions. As illustrated in Fig. 6a, the research workflow comprises four main stages: (1) structural digitization, where BSEAs, boronic acids, and selenylation products are converted to SMILES strings; (2) chemical fingerprint encoding (Fig. 6c), in which molecular structures are represented using molecular additive fingerprints (MAFs) to capture global molecular features and differential MAF (DiffMAF) fingerprints to emphasize the electronic environment around the Se(II) center;[51–53] (3) model development and

evaluation, where machine learning models are trained on these fingerprints to predict absolute yields and perform categorical classification of the selenylation reactions. The dataset is divided into a training set and a test set in an 8 : 2 ratio; (4) interpretation, where principal component analysis (PCA) is performed to visualize data clusters and identify structural features associated with high or low yields.[54–56]

To address the interpretability challenge in machine learning, we use PCA and visualization to analyze the model's learned abstract features in SeNEx reaction prediction. As shown in Fig. 6b, PCA reveals pronounced multi-cluster distributions that extend beyond simple steric considerations. High-yield reactions are clustered in the upper-left and lower regions, whereas low-yield reactions predominantly aggregate in the upper-right quadrant. Further inspection of representative reactants in high- and low-yield clusters highlights key structural trends: high-yield reactions are favored by N-substituents on BSEAs with low steric hindrance or aromatic moieties, and boronic acids are generally well tolerated (except for BA-6 and BA-20). Conversely, BSEAs bearing bulky substituents (such as Se-O and Se-P) exhibited diminished reactivity. To address these data characteristics, we propose a modular modeling framework: regression tasks are constructed to predict absolute yield values, while classification tasks grade reaction outcomes using threshold-based categories. Specifically, binary classification partitions the dataset into high and low yields at a 90% yield threshold, whereas ternary classification introduces an intermediate category, with thresholds set at 80% and 90%. Model assessment (Fig. 6d) demonstrates that the support vector machine (SVM) combined with MAF encoding attains 80% accuracy in binary classification, while NeuralNetTorch combined with DiffMAF encoding achieves 70% balanced accuracy in ternary classification. For regression, support vector regression (SVR) combined with DiffMAF encoding delivers experimental-to-predicted yield correlations with a root mean square error (RMSE) of only 6.2%, fulfilling the requirements for rapid reaction outcome prediction in practical scenarios. Representative prediction distributions across the three tasks are displayed in Fig. 6e.

In addition, the DNA-encoded library (DEL), conceptualized by Lerner and Brenner in 1992,[57] has emerged as a prevalent technology in current drug discovery due to its merits of huge capacity, easy storage, and efficient screening.[50,58–61] Typically, DELs are constructed via 3 to 4 cycles of interactive enzymatic DNA encoding and on-DNA combinatorial synthesis.[62–65] As a result, the development of DNA-compatible reactions is one of the key tasks in DELs.[66–68] Although a set of DNA compatible reactions such as diarylether synthesis,[69] cross-coupling reaction,[70–75] C–H activation and functionalization,[76,77] photo-promoted reaction,[78,79] cycloaddition reaction,[80] and the on-DNA synthesis of privileged heterocycles[81–83] have been developed in the past few years, only a few good reactions have been used in DEL synthesis,[84] due to the highly functionalized and sensitive DNA barcodes, low reaction scale and highly diluted conditions.[75,80,85] Nevertheless, the mild and robust conditions and the excellent functional group tolerance of this Ag(I)
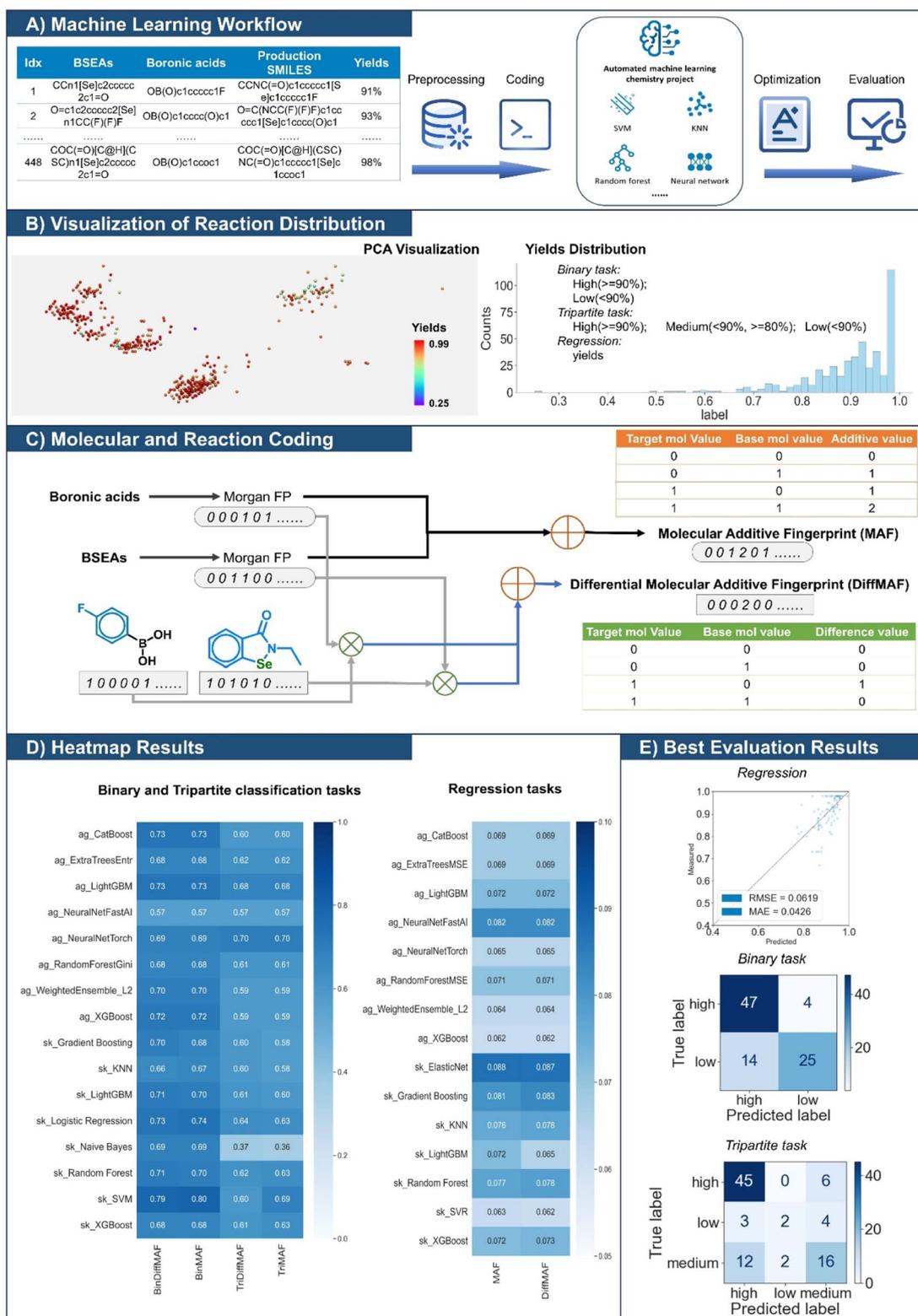
Fig. 6 (A) Workflow of the SeNEx-ML machine learning approach for selenylation reaction yield prediction. (B) Data visualization and distribution. Left: potential chemical space visualized by principal component analysis (PCA); right: data yield profiles and summary of ML tasks. (C) Schematic representation of MAF and DiffMAF fingerprint encoding. (D) Summary heatmap of various machine learning tasks, methods, and fingerprint encodings evaluated on the test set. Left: classification tasks (accuracy); right: regression task (RMSE). (E) Prediction results of the optimal models on the test set.

Fig. 7 Scope of the on-DNA SeNEx reaction of DNA-conjugated BSEAs and boronic acids. Standard reaction conditions: 1 equiv. of **HPi** (1 mM in ddH$_2$O), 10 equiv. of AgNO$_3$ (10 mM in ACN), 1000 equivalents of DIPEA (1 M in ACN), 1000 equiv. of boronic acid (1 M in ACN) in ACN−ddH$_2$O (6 : 1) 70 μL, rt, and 10 h. Conditions for on-DNA Suzuki cross-coupling: 1 equiv. of **D26** (1 mM in ddH$_2$O), 20 equiv. of PdCl$_2$(pph$_3$)$_2$ (10 mM in ACN), 600 equiv. of DIPEA (600 mM in ACN), 10 equiv. of KF (10 mM in ddH$_2$O), 500 equiv. of boronic acid (500 mM in ACN) in ACN−ddH$_2$O (1 : 1) 24 μL, 40 °C, and 2.5 h. The conversion of the on-DNA reactions was determined by LC-MS analysis. ACN, acetonitrile; ddH$_2$O, double distilled water.

catalyzed SeNEx chemistry indicate its potential for an ideal DNA-compatible reaction development.

To our delight, by using 20 equivalents of AgNO$_3$, 1000 equivalents of DIPEA, 1000 equivalents of boronic acid, and MeCN–ddH$_2$O (6 : 1) as solvents (SI, Table S2, entry 1), the on-DNA SeNEx reaction proceeded smoothly at room temperature, affording the desired DNA-conjugated selenide **D1** in 99% conversion (10 nmol scale), which was confirmed by the co-injection experiment (SI, Fig. S9). As delineated in Fig. 7, most of the tested boronic acids (multiple substitution types) reacted smoothly with DNA-conjugated BSEA **Hpi1** to produce the corresponding DNA-conjugated selenides in good to excellent conversions (**D1–D56**), except for DNA-conjugated selenides **D18** (46%), **D36** (52%), and **D56** (48%). Impressively, sterically hindered boronic acids (*e.g.*, 2-acetyl phenylboronic acid) are known to be inferior coupling partners in on-DNA Suzuki coupling.[74] However, in this on-DNA SeNEx reaction, a series of *ortho*-substituted boronic acids (**D2–D9**), including sterically hindered nitro (**D3**), acetyl (**D4**), methylsulfonyl (**D5**), iso-propoxyl (**D9**) and even 2,6-dimethyl substituted (**D35**) boronic acid, are all well tolerated (90–99%). Notably, apart from halo, alkyl, and alkyloxy groups, functional groups (FGs) including aldehyde (**D6, D39**), ketone (**D4**), nitro (**D3, D10, D23, D44, D56**), cyano (**D15, D24**), carboxy (**D27**), thiophene (**D29**), furan (**D30**), free indole (**D31**), quinoline (**D32**), carbazole (**D33**) and pyridine (**D34**) are all well compatible. Besides, the on-DNA parallel synthesis between 9 DNA-conjugated BSEAs and 4 representative boronic acids (NO$_2$, CN, CF$_3$, and OCH$_3$) also proceeded well, delivering the target selenides (**D57–D92**) in 80–99% conversions. Among the 92 tested on-DNA SeNEx reactions, 75 (82%) attained greater than 90% conversion, and 87 (95%) reached greater than 80% conversion. Moreover, a mock DEL construction was performed by using 3 cycles of chemistry including amidation, SeNEx, and Suzuki coupling. The desired conjugates **D93–D96** were obtained in 63–85% conversions over 3 steps on-DNA synthesis. More importantly, the gel electrophoresis analysis of the enzymatic ligation of **D1** with a 50-basepair primer showed complete ligation (SI, Fig. S10), and the qPCR results revealed that a DEL library has *ca.* 86% remaining amplifiable material under this DNA compatible SeNEx reaction, which is much higher than the threshold (30%) for practical DEL synthesis[86] (SI, Fig. S11). In addition, we further conducted two sets of $1 \times 2 \times 2$ (Fig. S12) and one set of $1 \times 2 \times 3$ (Fig. S21) mock library synthesis,[79] both using 3 cycles of chemistry including amidation, amidation and SeNEx chemistry. UPLC-MS data verified the structures of all corresponding members. Overall, this SeNEx click chemistry is a paradigm of both reaction-centric and product-centric on-DNA synthesis that features broad substrate scope and satisfactory DNA compatibility. Thus, it will have great application prospects in the synthesis of SeDEL for probing ultra-large Org-Se chemical world.

Conclusion

In summary, we have successfully designed and developed an unprecedented highly selective, and multi-orthogonal SeNEx chemistry (Se–N to Se–C(sp^2)) between BSEAs and boronic acids. This chemistry features modular, predictable, robust, high-yielding characteristics (>70% yield or conversion in 95% of 485 examples), proceeds under mild and switchable reaction conditions, and is operationally simple (tolerant to air and water). Impressively, this reaction demonstrates exceptional chemo-selectivity for Se–N over a wide range of competitive electrophiles, including –CHO, ketone, –SO$_2$F, S–N, –NO$_2$, –N$_3$, –CN, and ester. Furthermore, it tolerates a broad scope of transformable handles such as –COOH, –OH, –NH$_2$, amides, sulfonamides, and N-unprotected heterocycles. The excellent functional group compatibility enables this chemistry to be orthogonal to nearly the top 20 reactions in medicinal chemistry, as well as SuFEx, RuAAC, and CuAAC click chemistries, facilitating sequential and programmable synthesis of advanced Org-Se compounds. Due to these remarkable merits, this chemistry has been successfully applied in the late-stage modification of natural products, peptide modification/ligation, synthesis of Se-analogs of the marketed drug axitinib, sequential click chemistry (coupled with clickable C3–H selenylation of indole, SuFEx, RuAAC, and CuAAC), and protecting group-free syntheses of sequence-defined oligo selenides (non-amers). Additionally, this SeNEx chemistry demonstrates outstanding performance in on-plate nanomole-scale parallel synthesis (16×24) to afford a library of 384 selenides, with >70% conversion achieved in 368 cases (95.8%), indicating its suitability for *in situ* biological screening. Moreover, it performs effectively in DNA-encoded library synthesis (92 examples). Notably, a target-based screening identified **SA-16** as a potent CA XII inhibitor, with an IC$_{50}$ value of 72 nM. Furthermore, a machine learning-based model (SeNEx-ML) was established for reaction yield prediction, achieving 80% accuracy in binary classification and 70% balanced accuracy in ternary classification. These results demonstrated that this chemistry serves as a powerful tool to bridge the selenium chemical space with the existing chemical world, offering transformative potential in multidisciplinary fields, such as synthetic chemistry, material science, chemical biology, and medical chemistry.

Author contributions

W. H., H. X., and P. M. conceived the project and designed the experiments. W. Z., Y. W., S. Z., and J. P. performed the experiments and interpreted the data. S. H. assisted with the substrate scope investigation and programmable synthesis. S. Z. assisted with the late-stage natural product and peptide modification. C. Z. and A. S. assisted with machine learning research. S. Z., J. L., Y. Y., and P. M. assisted with the DNA-encoded substrate synthesis and parallel library construction. W. H., H. X., P. M., and A. S. wrote the manuscript with input from all authors, and all authors edited the manuscript.

Conflicts of interest

The authors declare no other competing interests.

Data availability

CCDC 2325780 contains the supplementary crystallographic data for this paper.[87]

The data that support the findings of this study are available in the supplementary information (SI) of this article. Supplementary information: materials and methods, experimental procedures, characterization data, and NMR and MS spectra. See DOI: https://doi.org/10.1039/d5sc05512a.

Acknowledgements

References

1 H. J. Reich and R. J. Hondal, *ACS Chem. Biol.*, 2016, **11**, 821–841.

2 C. M. Weekley and H. H. Harris, *Chem. Soc. Rev.*, 2013, **42**, 8870–8894.

3 S. Kumar, J. Yan, J. F. Poon, V. P. Singh, X. Lu, M. Karlssonott, L. Engman and S. Kumar, *Angew. Chem., Int. Ed.*, 2016, **55**, 3729–3733.

4 D. Bartolini, L. Sancineto, A. Fabro de Bem, K. D. Tew, C. Santi, R. Radi, P. Toquato and F. Galli, *Adv. Cancer Res.*, 2017, **136**, 259–302.

5 F. Cai, J. Zhang, H. Li, J. Dong, P. Xie, H. He, J. Guo, M. Chen, L. Xu, L. Ma and T. Chen, *Angew. Chem., Int. Ed.*, 2025, **64**, e202511720.

6 Z. Yang, D. Luo, C. Shao, H. Hu, X. Yang, Y. Cai, X. Mou, Q. Wu, H. Xu, X. Sun, H. Wang and W. Hou, *Eur. J. Med. Chem.*, 2024, **268**, 116207.

7 X. Deng, B. Xie, Q. Li, Y. Xiao, Z. Hu, X. Deng, P. Fang, C. Dong, H. B. Zhou and J. Huang, *J. Med. Chem.*, 2022, **65**, 7993–8010.

8 M. Rubio-Hernández, V. Alcolea, E. Barbosa da Silva, M. A. Giardini, T. H. M Fernandes, N. Martínez-Sáez, A. J. O'Donoghue, J. L. Siqueira-Neto and S. Pérez-Silanes, *J. Med. Chem.*, 2024, **67**, 19038–19056.

9 Y. Fu, R. Saxu, K. Ahmad Ridwan, C. Zhao, X. Kong, Y. Rong, W. Zheng, P. Yu and Y. Teng, *RSC Adv.*, 2022, **12**, 21821–21826.

10 W. Hou and H. Xu, *J. Med. Chem.*, 2022, **65**, 4436–4456.

11 W. Hou, H. Dong, X. Zhang, Y. Wang, L. Su and H. Xu, *Drug Discov. Today*, 2022, **27**, 2268–2277.

12 Y. Chen, H. Xu and W. Hou, *Future Med. Chem.*, 2025, **17**, 2281–2293.

13 W. M. Ching, *Proc. Natl. Acad. Sci. U. S. A.*, 1984, **81**, 3010–3013.

14 X. Zhang, F. Cheng, J. Guo, S. Zheng, X. Wang and S. Li, *Nat. Synth.*, 2024, **3**, 477–487.

15 I. P. Beletskaya and V. P. Ananikov, *Chem. Rev.*, 2022, **122**, 16110–16293.

16 S. Chen, C. Fan, Z. Xu, M. Pei, J. Wang, J. Zhang, Y. Zhang, J. Li, J. Lu, C. Peng and X. Wei, *Nat. Commun.*, 2024, **15**, 769.

17 J. Li, S. G. Ballmer, E. P. Gillis, S. Fujii, M. J. Schmidt, A. M. E. Palazzolo, J. W. Lehmann, G. F. Morehouse and M. D. Burke, *Science*, 2015, **347**, 1221–1226.

18 W. A. Golding, H. L. Schmitt and R. J. Phipps, *J. Am. Chem. Soc.*, 2020, **142**, 21891–21898.

19 G. J. Sherborne, A. G. Gevondian, I. Funes-Ardoiz, A. Dahiya, C. Fricke and F. Schoenebeck, *Angew. Chem., Int. Ed.*, 2020, **59**, 15543–15548.

20 Q. Xie and G. Dong, *J. Am. Chem. Soc.*, 2022, **144**, 8498–8503.

21 C. Yang, J. P. Flynn and J. Niu, *Angew. Chem., Int. Ed.*, 2018, **57**, 16194–16199.

22 P. H. S. Paioti, K. E. Lounsbury, F. Romiti, M. Formica, V. Bauer, C. Zandonella, M. E. Hackey, J. del Pozo and A. H. Hoveyda, *Nat. Chem.*, 2023, **16**, 426–436.

23 L. Cui, W. Hou and H. Xu, *Future Med. Chem.*, 2024, **16**, 493–496.

24 D. Shi, W. Liu, Y. Gao, X. Li, Y. Huang, X. Li, T. D. James, Y. Guo and J. Li, *Nat. Aging*, 2023, **3**, 297–312.

25 H. Jia, J. Han, Y. Qi, J. Liu, Y. Ting Leung, Y. H. Tung, Y. Chu, T. Wang, Y. M. E. Fung, Y. Wang and Y. Li, *Angew. Chem., Int. Ed.*, 2025, **64**, e202419904.

26 D. Feng, X. Li, J. Liu, X. Shao, L. Liu, Y. Shi, Y. Wang, M. Yu, S. Tang, L. Deng, Y. Zhang, S. Xie, J. Xu, S. Xu and H. Yao, *Chem. Sci.*, 2025, **16**, 15628–15637.

27 T. T. Ying, H. Q. Hu, X. W. Wu, X. L. Xu, J. Lv, S. N. Zhang, H. Wang, W. Hou, B. Wei and G. W. Rao, *Eur. J. Med. Chem.*, 2025, **290**, 117571.

28 F. Chen, Q. Liu, L. Ma, C. Yan, H. Zhang, Z. Zhou and W. Yi, *J. Med. Chem.*, 2025, **68**, 819–831.

29 W. Hou, Y. Zhang, F. Huang, W. Chen, Y. Gu, Y. Wang, J. Pang, H. Dong, K. Pan, S. Zhang, P. Ma and H. Xu, *Angew. Chem., Int. Ed.*, 2024, **63**, e202318534.

30 W. Hou, S. Hou, Y. Gu, S. Zhang, P. Ma, H. Y. Hu and H. Xu, *ChemBioChem*, 2024, **25**, E202400641.

31 W. Hou, X. Zhou, Z. Yang, H. Xia, Y. Wang, K. Xu, S. Hou, S. Zhang, D. Cui, P. Ma, W. Zhou and H. Xu, *Angew. Chem., Int. Ed.*, 2025, **64**, e202500942.

32 H. Xu, Y. Gu, S. Zhang, H. Xiong, F. Ma, F. Lu, Q. Ji, L. Liu, P. Ma, W. Hou, G. Yang and R. A. Lerner, *Angew. Chem., Int. Ed.*, 2020, **59**, 13273–13280.

33 H. Xu, Y. Wang, H. Dong, Y. Zhang, Y. Gu, S. Zhang, Y. Meng, J. Li, X. J. Shi, Q. Ji, L. Liu, P. Ma, F. Ma, G. Yang and W. Hou, *Angew. Chem., Int. Ed.*, 2022, **61**, e202206516.

34 Z. Zhou, Y. Gu, L. Wu, Y. Wang, H. Xu, L. Ma, Z. Zhang, J. Zhao, W. Zhang, W. Peng, G. Yang, X. Yu, H. Xu and W. Yi, *Chem*, 2023, **9**, 3335–3346.

35 D. T. Cohen, C. Zhang, B. L. Pentelute and S. L. Buchwald, *J. Am. Chem. Soc.*, 2015, **137**, 9784–9787.

36 C. S. Freitas, A. M. Barcellos, V. G. Ricordi, J. M. Pena, G. Perin, R. G. Jacob, E. J. Lenardão and D. Alves, *Green Chem.*, 2011, **13**, 2931–2938.

37 B. Goldani, V. G. Ricordi, N. Seus, E. J. Lenardão, R. F. Schumacher and D. Alves, *J. Org. Chem.*, 2016, **81**, 11472–11476.

38 N. Mukherjee, D. Kundu and B. C. Ranu, *Adv. Synth. Catal.*, 2017, **359**, 329–338.

39 Q. F. Xu-Xu, Y. Nishii, Y. Uetake, H. Sakurai and M. Miura, *Chem.–A Eur. J.*, 2021, **27**, 17952–17959.

40 V. V. Rostovtsev, L. G. Green, V. V. Fokin and K. B. Sharpless, *Angew. Chem., Int. Ed.*, 2002, **41**, 2596–2599.

41 J. Dong, L. Krasnova, M. G. Finn and K. B. Sharpless, Sulfur(VI) Fluoride Exchange (SuFEx): Another GoodReaction for Click Chemistry, *Angew. Chem., Int. Ed.*, 2014, **53**, 9430–9448.

42 D. G. Brown and J. Boström, *J. Med. Chem.*, 2016, **59**, 4443–4458.

43 A. B. Santanilla, E. L. Regalado, T. Pereira, M. Shevlin, K. Bateman, L. Campeau, J. Schneeweis, S. Berritt, Z. Shi, P. Nantermet, Y. Liu, R. Helmy, C. J. Welch, P. Vachal, I. W. Davies, T. Cernak and S. D. Dreher, *Science*, 2015, **347**, 443–448.

44 A. Osipyan, S. Shaabani, R. Warmerdam, S. V. Shishkina, H. Boltz and A. Dömling, *Angew. Chem., Int. Ed.*, 2020, **59**, 12423–12427.

45 M. Yang, M. K. Lee, S. Gao, L. Song, H. Y. Jang, I. Jo, C. C. Yang, K. Sylvester, C. Ko, S. Wang, B. Ye, K. Tang, J. Li, M. Gu, C. E. Müller, N. Sträter, X. Liu, M. Kim and P. Zhan, *Adv. Sci.*, 2024, **11**, 2404884.

46 N. Gesmundo, K. Dykstra, J. L. Douthwaite, Y. T. Kao, R. Zhao, B. Mahjour, R. Ferguson, S. Dreher, B. Sauvagnat, J. Saurí and T. Cernak, *Nat. Synth.*, 2023, **2**, 1082–1091.

47 G. Meng, T. Guo, T. Ma, J. Zhang, Y. Shen, K. B. Sharpless and J. Dong, *Nature*, 2019, **574**, 86–89.

48 S. C. Wang, X. Zhou, Y. X. Li, C. Y. Zhang, Z. Y. Zhang, Y. S. Xiong, G. Lu, J. Dong and J. Weng, *Angew. Chem., Int. Ed.*, 2024, **63**, e202410699.

49 C. T. Supuran, *Expert Opin. Investig. Drugs*, 2018, **27**, 963–970.

50 N. Favalli, G. Bassi, C. Pellegrino, J. Millul, R. De Luca, S. Cazzamalli, S. Yang, A. Trenner, N. L. Mozaffari, R. Myburgh, M. Moroglu, S. J. Conway, A. A. Sartori, M. G. Manz, R. A. Lerner, P. K. Vogt, J. Scheuermann and D. Neri, *Nat. Chem.*, 2021, **13**, 540–548.

51 J. Qiu, J. Xie, S. Su, Y. Gao, H. Meng, Y. Yang and K. Liao, *Chem*, 2022, **8**, 3275–3287.

52 J. Qiu, Y. Xu, S. Su, Y. Gao, P. Yu, Z. Ruan and K. Liao, *Chinese J. Chem.*, 2023, **41**, 143–150.

53 Y. Gao, K. Hu, J. Rao, Q. Zhu and K. Liao, *ACS Catal.*, 2024, 18457–18468.

54 R. Gómez-Bombarelli, J. N. Wei, D. Duvenaud, J. M. Hernández-Lobato, B. Sánchez-Lengeling, D. Sheberla, J. Aguilera-Iparraguirre, T. D. Hirzel, R. P. Adams and A. Aspuru-Guzik, *ACS Cent. Sci.*, 2018, **4**, 268–276.

55 N. Brown, P. Ertl, R. Lewis, T. Luksch, D. Reker and N. Schneider, *J. Comput. Aided. Mol. Des.*, 2020, **34**, 709–715.

56 A. Su and K. Rajan, *Sci. Data*, 2021, **8**, 1–10.

57 S. Brenner and R. A. Lerner, *Proc. Natl. Acad. Sci. U. S. A.*, 1992, **89**, 5381–5383.

58 P. Ma, S. Zhang, Q. Huang, Y. Gu, Z. Zhou, W. Hou, W. Yi and H. Xu, *Acta Pharm. Sin. B*, 2024, **14**, 492–516.

59 S. Wang, X. Shi, J. Li, Q. Huang, Q. Ji, Y. Yao, T. Wang, L. Liu, M. Ye, Y. Deng, P. Ma, H. Xu and G. Yang, *Adv. Sci.*, 2022, **9**, 2201258.

60 J. Xie, S. Wang, P. Ma, F. Ma, J. Li, W. Wang, F. Lu, H. Xiong, Y. Gu, S. Zhang, H. Xu, G. Yang and R. A. Lerner, *iScience*, 2020, **23**, 101197.

61 P. Ma, H. Xu, J. Li, F. Lu, F. Ma, S. Wang, H. Xiong, W. Wang, D. Buratto, F. Zonta, N. Wang, K. Liu, T. Hua, Z. Liu, G. Yang and R. A. Lerner, *Angew. Chem., Int. Ed.*, 2019, **58**, 9254–9261.

62 Y. Huang, Y. Li and X. Li, *Nat. Chem.*, 2022, **14**, 129–140.

63 M. Dockerill and N. Winssinger, *Angew. Chem., Int. Ed.*, 2023, **62**, e202215542.

64 A. Dixit, H. Barhoosh and B. M. Paegel, *Acc. Chem. Res.*, 2023, **56**, 489–499.

65 D. Neri and R. A. Lerner, *Annu. Rev. Biochem.*, 2018, **87**, 479–502.

66 W. Hou, S. Zhang, W. Yi, P. Ma and H. Xu, *Trends Chem.*, 2025, 7, DOI: 10.1016/j.trechm.2025.08.008.

67 K. Pan, Y. Yao, W. Bi and H. Xu, *Org. Lett.*, 2025, **27**, 10582–10587.

68 G. Zhao, M. Zhu, P. He, Q. Nie, Y. Li, G. Zhang and Y. Li, *Angew. Chem., Int. Ed.*, 2025, **64**, e202507064.

69 H. Xu, T. Tan, Y. Zhang, Y. Wang, K. Pan, Y. Yao, S. Zhang, Y. Gu, W. Chen, J. Li, H. Dong, Y. Meng, P. Ma, W. Hou and G. Yang, *Adv. Sci.*, 2022, **9**, 2202790.

70 H. Xu, F. Ma, N. Wang, W. Hou, H. Xiong, F. Lu, J. Li, S. Wang, P. Ma, G. Yang and R. A. Lerner, *Adv. Sci.*, 2019, **6**, 1901551.

71 Y. Zhang, W. Chen, T. Tan, Y. Gu, S. Zhang, J. Li, Y. Wang, W. Hou, G. Yang, P. Ma and H. Xu, *Chem. Commun.*, 2021, **57**, 4588–4591.

72 F. Ma, J. Li, S. Zhang, Y. Gu, T. Tan, W. Chen, S. Wang, H. Xu, G. Yang and R. A. Lerner, *ACS Catal.*, 2022, **12**, 1639–1649.

73 X. Li, J. Zhang, C. Liu, J. Sun, Y. Li, G. Zhang and Y. Li, *Chem. Sci.*, 2022, **13**, 13100–13109.

74 Y. Ding, J. L. DeLorey and M. A. Clark, *Bioconjug. Chem.*, 2016, **27**, 2597–2600.

75 D. T. Flood, S. Asai, X. Zhang, J. Wang, L. Yoon, Z. C. Adams, B. C. Dillingham, B. B. Sanchez, J. C. Vantourout, M. E. Flanagan, D. W. Piotrowski, P. Richardson, S. A. Green, R. A. Shenvi, J. S. Chen, P. S. Baran and P. E. Dawson, *J. Am. Chem. Soc.*, 2019, **141**, 9998–10006.

76 H. Xu, W. Chen, M. Bian, H. Xu, H. Gao, T. Wang, Z. Zhou and W. Yi, *ACS Catal.*, 2021, **11**, 14694–14701.

77 S. Zhang, H. Zhang, X. Liu, P. Qi, T. Tan, S. Wang, H. Gao, H. Xu, Z. Zhou and W. Yi, *Adv. Sci.*, 2024, **11**, 2307049.

78 J. P. Phelan, S. B. Lang, J. Sim, S. Berritt, A. J. Peat, K. Billings, L. Fan and G. A. Molander, *J. Am. Chem. Soc.*, 2019, **141**, 3723–3732.

79 J. Zhang, J. Liu, X. Li, Y. Ju, Y. Li, G. Zhang and Y. Li, *J. Am. Chem. Soc.*, 2024, **146**, 2122–2131.

80 M. V. Westphal, L. Hudson, J. W. Mason, J. A. Pradeilles, F. J. Zécri, K. Briner and S. L. Schreiber, *J. Am. Chem. Soc.*, 2020, **142**, 7776–7782.

81 J. Zhang, X. Li, H. Wei, Y. Li, G. Zhang and Y. Li, *Org. Lett.*, 2021, **23**, 8429–8433.

82 H. Xiong, Y. Gu, S. Zhang, F. Lu, Q. Ji, L. Liu, P. Ma, G. Yang, W. Hou and H. Xu, *Chem. Commun.*, 2020, **56**, 4692–4695.

83 K. Pan, Y. Yao, Y. Zhang, Y. Gu, Y. Wang, P. Ma, W. Hou, G. Yang, S. Zhang and H. Xu, *Bioconjug. Chem.*, 2023, **34**, 1459–1466.

84 P. R. Fitzgerald and B. M. Paegel, *Chem. Rev.*, 2021, **121**, 7155–7177.

85 Q. Huang, Y. Gu, A. Qin, P. Ma, H. Xu and S. Zhang, *ACS Med. Chem. Lett.*, 2024, **15**, 1591–1597.

86 H. Wang, G. Zhao, T. Zhang, Y. Li, G. Zhang and Y. Li, *ACS Pharmacol. Transl. Sci.*, 2023, **6**, 1724–1733.

87 Deposition number 2325780 (**52**) contain the supplementary crystallographic data for this paper. These data are provided free of charge by the joint Cambridge Crystallographic Data Centre and Fachinformationszentrum Karlsruhe via, **http://www.ccdc.cam.ac.uk/structures**, DOI: **10.5517/ccdc.csd.cc2j255**.